IEEE Access
Multidisciplinary | Rapid Review | Open Access Journal

Received October 21, 2017, accepted December 23, 2017, date of publication January 3, 2018,
date of current version February 28, 2018.

Digital Object Identifier 10.1109/ACCESS.2017.2787684

Robust Interference Cancellation of Chirp and CW Signals for Underwater Acoustics Applications

ROEE DIAMANT
Department of Marine Technology, University of Haifa, Haifa 3498838, Israel
roeed@univ.haifa.ac.il

This work was supported in part by the European Union's Horizon 2020 research and innovation program under Grant 773753 (Symbiosis) and in part by the NATO Science for Peace and Security Program under Grant G5293.

ABSTRACT We focus on mitigating strong interferences that can jam underwater acoustics emissions aimed for detection or communications. We consider two types of interferences: narrowband like continuous waveform and wideband like chirp. Both the types are assumed to be strong, such that, without interference cancellation, performance is poor. We offer two interference canceling algorithms, each corresponding to a different interference type. The two algorithms are designed to mitigate strong interference, while maintaining the desired signal intact. These algorithms can be executed sequentially to manage both types of interference simultaneously. Our solution takes advantage of the sparsity of the underwater acoustic channel, as well as the assumed correlation of the interference signals. Numerical simulations, as well as results from a sea experiment, show that our algorithms significantly reduce the effect of strong interferences for the fast time-varying and long-delay spread underwater acoustic channel.

INDEX TERMS Underwater acoustic communication, underwater signal detection, interference canceling, noise canceling, single carrier interference, wideband interference.

I. INTRODUCTION

Underwater acoustics is required for a multitude of applications such as oceanographic data collection, warning systems, periodic sampling of water quality, identification of sounds from marine mammals, as well as a means for underwater communication [1]. In some of these applications, the signals are recorded in harsh environments, such as closed harbors or near noisy vessels. These environments pose the challenge of signal processing in the presence of strong interferences [2]. If the reception is interfered with by acoustic emissions within the same frequency band as that of the desired signal, the signal-to-interference-plus-noise (SINR) is likely to be low and performance will greatly decrease. It is therefore good practice to employ a noise-canceling filter as a first step in the reception chain [3]. The aim of this work is to describe our robust design for such a filter.

The challenge of interference cancellation (IC) should be treated for both a single carrier interference, like continuous waveform (CW) signals, and for a wideband interference, like chirp signals. An example of the former is acoustic noise from vessels' ignition systems; an example of wideband interference can be the short pulses of echo-sounders or chirp signals from sonar systems [4]. We do not assume prior information about the interference type. Thus, the solution for IC should be capable of managing both types of interferences. As illustrated in Fig. 1, our solution combines the mitigation of narrowband interference and wideband interference. We aim to mitigate these interferences as much as possible by avoiding the distortion of the desired signal. Regarding narrowband interference, we assume the interference is correlated over time and of an unknown frequency. In the case of wideband interference, we assume that the wideband interference's structure is known (or can be estimated).

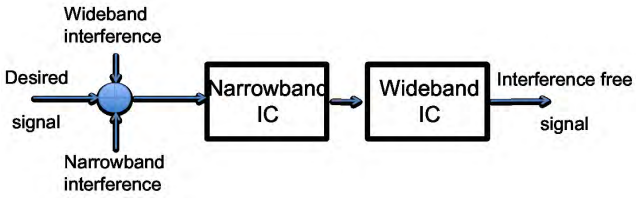

FIGURE 1. System diagram.

The application of IC for radio frequency (e.g., [5]) cannot be directly adopted for underwater acoustics. This is because of the channel's non-stable frequency response

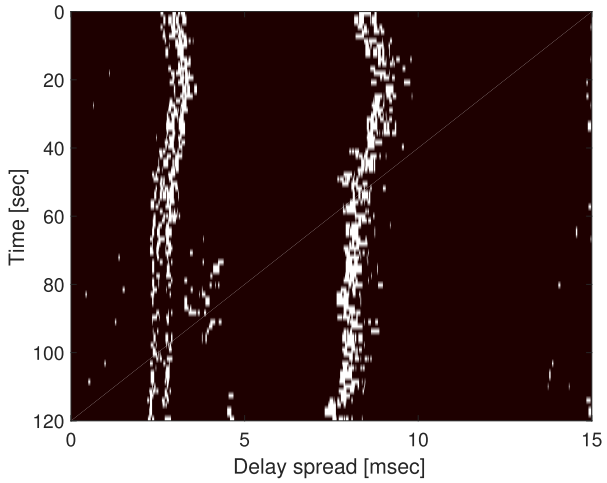

FIGURE 2. An example of a time-varying underwater acoustics channel impulse response collected during our sea experiments. The channel was measured for a receiver deployed in 10 m of water, and a transmitter in 35 m of water. Water depth was 125 m. The rows of the illustrated matrix represent the time sequence of the channel's impulse response. We observe two main time-varying reflections, and a delay spread of about 10msec.

caused by the time-varying multipath channel, and the channel's much shorter coherence time [6]. While IC solutions for underwater acoustic interferences have been proposed before (e.g., [7], [8]), these studies mainly considered the mitigation of strong interference types and were not designed to avoid the distortion of the desired signal. Moreover, the available solutions for underwater acoustics require a long convergence time. This is mainly due to the need to track the underwater acoustic channel, which is characterized by a long delay spread and is modelled as a tap delay line of hundreds of taps [6]. These channel characteristics are demonstrated in Fig. 2. The figure shows an example of a time-varying normalized channel impulse response evaluated from recordings collected during our sea experiment. A long delay spread of 25 ms with significant changes over time is observed.

Our IC solution is a combination of two fast-converging algorithms. The first, referred to as the *single-carrier IC* (SC-IC) algorithm, is designed to mitigate strong correlative narrowband components between a reference buffer from the channel, containing only the interference, and a buffer containing both the interference and desired signals. To be initialized, the algorithm requires at least one reference block from the channel that does not include the desired signal. It then proceeds by employing IC over consecutive time windows. In this way, the algorithm can easily adapt to changes in the interference signal's structure. Still, we allow for the option of a filter's memory to improve IC for stable interferences. The fast convergence of SC-IC is due to its efficient implementation in the frequency domain. Our second IC algorithm, referred to as the *wideband IC* (WB-IC) algorithm, aims to mitigate strong wideband interference originating from a transmitter located close to the receiver. Assuming knowledge of this interference's signal structure, we take an adaptive noise-canceling (NC) approach, whose uniqueness is in the guidance of the NC adaptive filter towards the interference's significant channel taps. This allows us to achieve two goals: a fast convergence, since the channel equalizer does not need to track the full channel, and avoiding the distortion of the desired signal, since the adaptive NC filter avoids tracking the taps of that signal.

To summarize, the contribution of this work is threefold:

1) A fast convergence IC algorithm for strong single-carrier underwater acoustic interferences.
2) A fast convergence IC algorithm for strong wideband underwater acoustic interferences.
3) An holistic framework that serves as a first step in the reception chain for mitigation of interferences with a small distortion of the desired signal.

Our two IC solutions can perform without distorting the desired signal noticeably, both in the presence of an interference or in its absence. This property allows for the application of the two algorithms sequentially, thereby simultaneously managing the two interference types. Simulation results for CW interferences and for chirp interferences show that our two IC solutions mitigate strong interferences by as much as 40 dB, without distorting the desired signal noticeably. To demonstrate our two algorithms, we show results from a sea experiment, showing similar behavior in a real shallow and deeper water sea environment.

The remainder of this paper is organized as follows. The state-of-the-art in IC for underwater acoustics is discussed in Section II. Our system model and main assumptions are listed in Section III. The details of the SC-IC and WB-IC are presented in Section IV. Next, performance evaluation via numerical simulation (Section V-A) and the results of a sea experiment (Section V-B) are presented in Section V. Finally, conclusions are drawn in Section VI.

II. STATE-OF-THE-ART

Underwater acoustics is inherently challenging, due to the dispersive nature of most realistic underwater acoustic channels. These channels are typically characterized by rapid time-varying multipath propagation, path-dependent Doppler shifts, and significant delay-Doppler spread [9]. For example, for underwater acoustic communication (UWAC) applications, in order to set up coherent point-to-point communications that achieves sufficiently high (order-of kbps) bit rates, adaptive equalization is required [10]. Turbo equalization for UWAC also attracts a lot of interest [11], as it is well suited to long reverberating channels and achieves a high data rate over long distances [12]. The long delay spread and fast time-variability of the underwater channel often makes the precise design of adaptive filters prohibitively complex from a computational point of view.

While equalization techniques and channel compensation for underwater acoustics have been widely explored, little has been done to combat strong non-Gaussian interference. The considered interferences can be divided into three classes:

1) Short-term noise transients and small bandwidths, which are mostly induced by snapping shrimps and rain;

2) Man-made narrowband signals of long duration like CW signals;
3) and sonar and communication-based periodic wideband signals like chirps.

For the first type of interference, IC is mostly handled in the framework of a channel coding scheme, e.g., [13], [14]. In [15], a nulling approach for noise transient cancellation is performed, where impulsive signals are identified based on Doppler shift estimation. In [16], noise transients are identified by comparing the output of two successive channel estimations. The authors of [8] introduced a wavelet-based filtering technique, which is also able to reduce the effect of the noise transient in high frequency bands, while smoothing the output of the wavelet denoising. In this paper, the proposed solution considers the last two interference types.

Since stationary interferences of the second type greatly interfere with modern communication techniques, such as orthogonal-frequency-division-multiplexing (OFDM), there are many possible solutions for mitigating such interferences for radio frequency communications. Most of these focus on estimating the interference parameters, e.g., [17], or on spatial reuse techniques, e.g., [18]. Yet, the joint assumption is of a slow, time-varying channel. For fast time-varying underwater acoustic channels with interference of the second type, [19] described a decoding process that uses prior information about the interference structure. The decoding uses the detected interference within the iterative framework of the generalized likelihood ratio test. Yet, the time duration of the interference is considered shorter than the desired signal.

The time-varying characteristics of the underwater acoustic channel dictates the use of adaptive filters for IC. The noise canceling (NC) filter includes an adaptive filter, which receives a synthetic template of the interference signal as a reference. The output of this filter is then removed from the channels' received signal, and the outcome is the noise-free signal. The general setting of such an NC filter is illustrated in Fig. 3.

A good survey of possible adaptive filters suitable for NC is available in [20]. In [7], the authors considered the potential of improving communications performance by canceling mutual interferences from multiple transmitters. To speed up convergence, instead of using adaptive equalization, cancellation is achieved through the time reversal technique. Yet, time reversal assumes a symmetrical and stable channel, which is a hard assumption for underwater acoustic channels. Regarding the aim of channel estimation in the context of IC, a comparison was made in [21] between the recursive least square (RLS), and the matching pursuit algorithm, whose implementation is described in [22]. The analysis also considered the effect of the Doppler shift. It was shown that enhanced IC is obtained using the matching pursuit algorithm, but at the cost of convergence time. Managing the fast time-varying channel to mitigate interference signals of types (2) and (3) is the focus of our work.

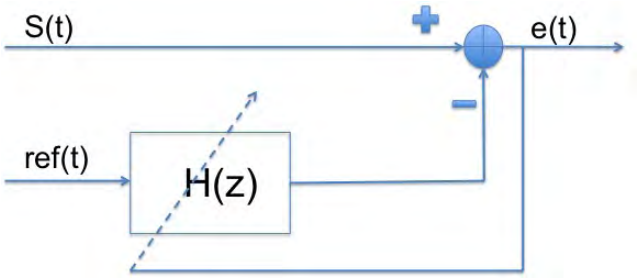

FIGURE 3. Diagram of the noise cancellation filter.

III. SYSTEM MODEL

Our system's setup includes a desired source whose acoustic emissions are received by submerged receiver. The emissions take place in a harsh environment with many man-made interferences. This can be a harbor environment or an area with significant shipping activity. The receiver overhears the desired signal with the addition of an interference. The considered interference types can be a continuous narrowband single carrier, a wideband interference signal of finite duration, or both interference types simultaneously. An example of a narrowband interference type is the signals produced by a ship's motor, while an example of wideband interference can be a chirp signal or a short pulse generated by the sonar system or the echo-sounder of a nearby vessel.

A. MAIN ASSUMPTIONS

We assume spatial processing is not possible. That is, the transmitter has a single omnidirectional projector, and the receiver has a single omnidirectional hydrophone. The received desired signal is assumed to be of high signal to noise ratio (SNR), but also of high initial interference-to-signal ratio (ISR). We assume that either no interference exists, or both or one of the two types of interferences exist. Both interrupting signals are assumed to lie within the frequency band of the desired signal, and well within the duration of the desired signals. Without IC, the expected effect is therefore a failure to detect/decode the desired signal. Still, the interference signal is assumed not to correlate well with the desired signal.

In mitigating a narrowband interference, we do not assume to have prior knowledge of the interference signal's structure. This is because we consider narrowband interferences that have a random appearance, e.g., from the motors of passing ships of an unknown type. Yet, although we assume a buffer containing the interference signal, we do not assume the desired signal can be identified. We refer to this buffer as the *reference buffer*. The identification of the reference buffer is possible, considering that the interference and desired signals are probably only partly aligned in the time domain. We assume the interference affecting the desired signal has a high correlation with the interference contained in the reference buffer.

In contrast to narrowband interference, we assume the wideband interference structure is known or well estimated.

This includes the bandwidth, duration, and modulation form of the interfering signal. This case applies when the interference originates from a devise whose parameters are known to the receiver. For example, a nearby node in a communication network, an ecosounder, or a sonar system. While interference signal estimation is beyond the scope of this work, it is clear that detection and estimation of the interference signal are possible when the SNR and ISR are high, and when the interference is transmitted periodically in the channel. In these conditions and when the SNR is large, the receiver can also estimate the Doppler shift experienced by the interference signal via e.g. [23]. However, the channel state information for the interfering signal is not known, and we pose no limitation for the arrival time of the interfering wideband signal, and it can be received either before or during the arrival of the desired signal. As in all equalization processes, our IC method for wideband interferences is sensitive to mismatches in the knowledge of the structure of the interference signal. However, small errors in the assumed duration and bandwidth of the signal are allowed. This is because, since the ultimate goal of the IC method is to mitigate the interference, small remains of interferences are tolerable.

For the aim of IC, while possibly known information about the modulation structure of the desired signal is available, this information is not used. This is due to the fact that the ISR is high; therefore, potential iterative decoding of the desired signal is not possible. That is, the entire interference should be mitigated to allow for proper decoding. We perform the IC at the very beginning of the reception chain. At this stage, we assume the underwater acoustic channel is unknown. Still, we assume the channel is fast time-varying, such that a fast convergence IC is required. As is customary for underwater acoustic channels, we assume the channel is of a very long delay spread, such that a brute-force equalization of the interrupting signal is extremely challenging. However, we assume the multipath channel is sparse and comprised of only a few significant arrivals. While the structure of the desired signal may sometimes be the same as that of the interfering signal, since it is unlikely that the arrival time of the desired signal will exactly match the arrival of the interrupting signal, we assume these significant arrivals are not aligned with that of the desired signal.

B. QUALITY MEASURES

Our goal is to design an IC filter to mitigate both narrowband and wideband interferences. To this end, we measure performance in terms of the SINR difference after and before the IC, ρ_{power}. For narrowband interference, we measure ρ_{power} in the frequency domain and are limited by the power of the desired signal (i.e., until the interference-to-signal ratio is 1). For the wideband signal, we estimate ρ_{power} by comparing the output of the matched filter for both the desired signal and the interference signal.

Since we are also interested in avoiding the desired signal's distortion, we adopt the normalized matched filter (NMF) [24],

$$\text{NMF} = \frac{\int s(t)y(t)dt}{\sqrt{\int s^2(t)dt \int y^2(t)dt}}, \tag{1}$$

where $s(t)$ and $y(t)$ are the template and received signals, respectively. We use the NMF as a test to show the amount of distortion a signal experiences before and after the IC. For example, since the wideband interference signal is strong, assigning $s(t)$ as the interference signal, we expect to obtain a high MF value before the IC, but a low one after the IC. Alternatively, setting $s(t)$ as the desired signal, we expect a low NMF before the IC, but a high MF value after it. Denoting $\text{NMF}^{\text{before}}(s(t))$ and $\text{NMF}^{\text{after}}(s(t))$ as the NMF output matched to signal $s(t)$ before and after the IC, respectively, we measure performance in terms of the ratio

$$\rho_{\text{distort}}(s(t)) = \frac{\text{NMF}^{\text{after}}(s(t))}{\text{NMF}^{\text{before}}(s(t))}. \tag{2}$$

IV. PROPOSED IC METHODS

In this section, we present our SC-IC and WB-IC methods. For both methods, we use the IC framework illustrated in Fig. 3. The framework is comprised of a reference interference signal, $\boldsymbol{r}$, passing through an adaptive filter, whose aim is to estimate the channel impulse response experienced by the interference signal. The output of the adaptive filter is subtracted from the signal coming from the channel, $\boldsymbol{s}$. The result is used as feedback for the adaptive filter, and is treated as an interference-free signal. In the following, we describe the operation of the SC-IC and WB-IC algorithms in detail.

A. IC FOR SINGLE-CARRIER INTERFERENCES: SC-IC

Recall that for narrowband interference mitigation, we assume the existence of a reference buffer containing an interference that is highly correlated with the interference affecting the desired signal. We refer to the latter buffer from the channel as the *signal buffer*. Referring to Fig. 3, we use this reference buffer as the reference signal. The main idea is to utilize the knowledge that the interference is narrowband, and to perform the IC operation only for those frequency bands that are affected by the interfering signal. The other frequency bands are not affected, thereby reducing the distortion level of the desired signal. The identification of the frequency bands dominated by the interference is performed by tracking the covariance matrix of the adaptive filter's error signal in the frequency domain.

Let A be the order of the adaptive filter. Also let B be the number of samples in the reference buffer. For simplicity, $N = B/A$ is assumed to be an integer value. The SC-IC algorithm divides the signal and reference vectors into N time windows. The following is performed for each such time window n.

The algorithm uses the normalized least mean square (NLMS) as the adaptive filter, and works in the frequency domain to improve efficiency. Let α and γ be the adaptation and leakage factors (we used 0.05 and 0.999),

respectively. Also let $\boldsymbol{S}_n$ and $\boldsymbol{R}_n$ be the frequency representation of vectors of N samples corresponding to the nth block of the signal buffer, $\boldsymbol{s}_n$, and the reference buffer, $\boldsymbol{r}_n$, respectively. To allow for a smooth transaction between adjacent filtered time windows, we extend $\boldsymbol{R}_n$ to also include the previous $n-1$ time window from the reference buffer. The frequency representation of the adaptive filter's weights is denoted by $\boldsymbol{W}_n$, and the output of the IC is denoted by $\boldsymbol{E}_n$.

The adaptive filter's weights are determined by

$$\boldsymbol{W}_n = \gamma \boldsymbol{W}_{n-1} + 2\boldsymbol{\mu}_n \boldsymbol{E}_n \boldsymbol{R}_n^{\mathrm{H}}, \tag{3}$$

where $\boldsymbol{R}_n^{\mathrm{H}}$ is the conjugate transpose of $\boldsymbol{R}$, and $\boldsymbol{\mu}_n$ is the normalized step size. Let

$$\boldsymbol{k}_n = \frac{\alpha}{\boldsymbol{R}_n^{\mathrm{p}}},$$

where $\boldsymbol{R}_n^{\mathrm{p}}$ is the estimated power of the reference signal whose smooth estimate is

$$\boldsymbol{R}_n^{\mathrm{p}} = \Gamma \boldsymbol{R}_{n-1}^{\mathrm{p}} + (1-\Gamma)\boldsymbol{R}_n \boldsymbol{R}_n^{\mathrm{H}}, \tag{4}$$

and Γ is a normalized time constant (we use $\Gamma = 0.9$). To avoid divergence, the step size is limited using

$$\mu(i)_n = \begin{cases} k_n(i) & \text{if } k_n(i) < \min(\boldsymbol{k}_n) \times m \\ \min(\boldsymbol{k}_n) \times m & \text{otherwise,} \end{cases} \tag{5}$$

where m is the dynamic range of the step size (we use $m = 10000$). To calculate $\boldsymbol{E}_n$, we set

$$\boldsymbol{E}_n = \boldsymbol{S}_n - \boldsymbol{R}_n \times \boldsymbol{W}_n^{\mathrm{T}}. \tag{6}$$

The frequency domain NLMS in (3) gives extended weight to frequency bands of high power through the step size (6). Utilizing the correlation between the narrowband interference in the reference and signal buffers, we further modify the step size, such that

$$k_n(i) = \begin{cases} \dfrac{\alpha}{R^{\mathrm{p}}(i)_n} & \text{if } i \in \mathcal{C}^{\mathrm{s}} \\ 0 & \text{otherwise,} \end{cases} \tag{7}$$

where $\mathcal{C}^{\mathrm{s}}$ is a set of frequency indexes estimated to include the interference signal's energy. As a result, the subtraction in (6) is performed only for frequency bands including interferences. As we show in the performance analysis, this somewhat heuristic operation greatly improves performance. This is because, otherwise, out-of-band interferences may receive high weights and, as a result, wrongly dominate the filtering.

We find $\mathcal{C}^{\mathrm{s}}$ from (7) based on two criteria. The first is a comparison of the power $\boldsymbol{R}_n^{\mathrm{p}}$ with the signal buffer's power, calculated by

$$\boldsymbol{S}_n^{\mathrm{p}} = \Gamma \boldsymbol{S}_{n-1}^{\mathrm{p}} + (1-\Gamma)\boldsymbol{S}_n \boldsymbol{S}_n^{\mathrm{H}}. \tag{8}$$

Specifically, we look for frequency indexes i, for which $S_n^{\mathrm{p}}(i)/R_n^{\mathrm{p}}(i)$ is close to 1. The second is frequency indexes i for which the IC output, $E_n(i)$, monotonously declines with n. That is

$$E_n(i) < E_{n-1}(i) < E_{n-2}(i) < \ldots. \tag{9}$$

The rationale behind (9) is that looking at $\boldsymbol{E}_n$, over time, SC-IC should reduce the energy of the frequency bands that include narrowband interferences.

Note that SC-IC can make use of several reference buffers. To achieve this, we change the spectrum vector, $\boldsymbol{R}$, into a matrix whose rows correspond to different reference buffers. The filter output is now obtained by summing the rows of the filter for each reference buffer. This feature becomes handy when several narrowband signals interfere with decoding, such as the harmonics of a ship's motor.

The SC-IC algorithm can operate with and without memory. The former is employed by simply continuing to update the adaptive filter from the signal buffer's last time window to the first time window in the new signal buffer. Yet, to avoid distorting the desired signal, the reference buffer remains the same. This filter updating becomes handy when the signals are long or when the interference signal is assumed to always exist in the channel. In such cases, due to the time-varying channel, the IC must continuously estimate the channel. Still, as the results of our numerical simulations and experimental analysis show, the IC manages to greatly increase the SINR without distorting the desired signal noticeably. This is because it utilizes the fact that the interference signal is much stronger than the desired signal; thus, its channel estimate can be easily differentiated from that of the desired signal.

B. IC FOR WIDEBAND INTERFERENCES: WB-IC

In contrast to SC-IC, WB-IC is based on the RLS adaptive filter, whose basic equations for the nth time window are

$$\boldsymbol{k}_n = \frac{\Lambda^{-1}\boldsymbol{P}_{n-1}\boldsymbol{r}_n}{1 + \Lambda^{-1}\boldsymbol{r}_n^{\mathrm{T}}\boldsymbol{P}_{n-1}\boldsymbol{r}_n} \tag{10a}$$

$$\boldsymbol{e}_n = \boldsymbol{s}_n - \boldsymbol{r}_n^{\mathrm{T}}\boldsymbol{w}_{n-1} \tag{10b}$$

$$\boldsymbol{w}_n = \boldsymbol{w}_{n-1} + \boldsymbol{r}_n \boldsymbol{e}_n \tag{10c}$$

$$\boldsymbol{P}_n = \Lambda^{-1}\boldsymbol{P}_{n-1} - \Lambda^{-1}\boldsymbol{k}_n \boldsymbol{r}_n^{\mathrm{T}}\boldsymbol{P}_{n-1}, \tag{10d}$$

where $\boldsymbol{P}_n$ is the error covariance matrix, and Λ is a chosen scalar.

The task of mitigating wideband interferences is different than that of mitigating narrowband interferences. This is because of the long, fading underwater acoustic channel, which requires the estimation of sometimes hundreds of taps. Instead of equalizing the full channel, WB-SC makes use of the sparse nature of the channel to track only those significant channel taps that are related to strong interference. Other channel taps are then zero-forced. Consequently, the effective order of the adaptive filter becomes much smaller, and the efficiency of the equalization process greatly improves. By zero-forcing the non-significant taps, we also prevent the algorithm from overfitting the ambient noise or the desired signal as an interference. Otherwise, noise may be amplified, and the desired signal may be distorted. The details of the algorithm are presented below.

We start by identifying the channel taps that belong to the wideband interference. The location indexes of these taps are

placed in a set $\mathcal{C}^{\mathrm{w}}$, such that

$$\mathcal{C}^{\mathrm{w}} = \{l_1 - \Delta, \ldots, l_1, \ldots, l_1 + \Delta, \ldots, l_L - \Delta, \ldots, l_L, \ldots, l_L + \Delta\}, \quad (11)$$

where $l_1, \ldots, l_L$ are the locations of the identified taps comprising a set $\mathcal{L}$, and Δ is a measure of the uncertainty of the evaluated location for each channel tap.

To prepare set $\mathcal{L}$, we perform the NMF in (1) matched to the interference signal, and choose the locations of only those taps whose absolute value is higher than a threshold X_T chosen by [24]

$$P_{\mathrm{fa}} = 1 - B\left(x_T^2, \frac{1}{2}, \frac{N-1}{2}\right), \quad (12)$$

where P_{fa} is the required false alarm probability, and

$$B(a, b, z) = \int_0^a t^{b-1}(1-t)^{z-1} dt$$

is the regularized incomplete beta function. Note that (12) reveals the advantage of the NMF, which does not require calculating the noise characteristics for thresholding. The uncertainty parameter Δ in (11) is initialized proportionally to the ratio between the bandwidth of the interference signal, B_w, and an assumed coherence time, T_c, such that

$$\Delta_1 \propto \frac{1}{\mathrm{B_w} T_c}. \quad (13)$$

Δ_n is then adaptively evaluated by the variance of the locations in $\mathcal{L}$.

To direct the operation of the adaptive filter towards the mitigation of only the strong interference signal, we modify the RLS in (10) both during initialization and in steady state. Since the error covariance matrix is proportional to the covariance of the unknown filter's coefficients, its initialization is commonly determined as $\boldsymbol{P}_1 = c\boldsymbol{I}$ [3], where $\boldsymbol{I}$ is the identity matrix. Instead of zero-forcing outside the region of $\mathcal{C}^{\mathrm{w}}$, we set $\boldsymbol{P}_1 = c\boldsymbol{H}$, where

$$H(i,j) = \begin{cases} 0 & \text{if } i \neq j \\ 0 & \text{if } i = j,\ i \notin \mathcal{C}^{\mathrm{w}} \\ 1 & \text{otherwise,} \end{cases} \quad (14)$$

Similarly, while the filter weights are usually initialized as zeros, we set

$$w_0(i) = \begin{cases} 0 & \text{if } i \notin \mathcal{C}^{\mathrm{w}} \\ \hat{h}^{\mathrm{strong}}(i) & \text{otherwise,} \end{cases} \quad (15)$$

where vector $\hat{\boldsymbol{h}}^{\mathrm{strong}}$ is zero for all $i \notin \mathcal{C}^{\mathrm{w}}$, and otherwise equals the complex value of a significant path of the NMF, located closest to index i. For example, for all $i \in \mathcal{C}^{\mathrm{w}}$ indexes closest to $l_j \in \mathcal{L}$, we let $\hat{h}^{\mathrm{strong}}(i-\Delta), \ldots, \hat{h}^{\mathrm{strong}}(i+\Delta)$ equal the output of the NMF at l_j.

In its steady state, WB-IC updates the filter's weights by

$$w_n(i) = \begin{cases} 0 & \text{if } i \notin \mathcal{C}^{\mathrm{w}} \\ \boldsymbol{w}_{n-1} + \boldsymbol{r}_n \boldsymbol{e}_n & \text{otherwise.} \end{cases} \quad (16)$$

Convergence improves if we also zero-force

$$P_n(i,j) = 0 \quad \text{if } i \notin \mathcal{C}^{\mathrm{w}}, j \notin \mathcal{C}^{\mathrm{w}}. \quad (17)$$

V. PERFORMANCE ANALYSIS

In this section, we test our SC-IC and WB-IC performance methods. Results are shown for both synthetic signals and real signals recorded during a sea experiment. While there are several IC solutions for underwater acoustics, the available solutions require an acoustic array [2], [7], or only fit the case of either a balanced SINR [11], [19], [25], [26] or noise transients [8], [16]. Therefore, to test the performance of the proposed IC solution, the traditional noise cancellation (*NC*) filter in [27] is adopted as a benchmark. The NC implementation used is that of the MATLAB signal processing toolbox release ed. R2017a. For a fair comparison, we match the adaptive filter used by our IC and by NC. Results are shown for the SINR ratio, ρ_{power}, the signal distortion measure, $\rho_{\mathrm{distort}}(s(t))$ from (2), and the bit error rate.

A. NUMERICAL SIMULATIONS

1) SIMULATION SETUP

Our simulation setup is comprised of a sequence of JANUS-based communication signals [28] that serve as the desired signal. The JANUS system uses frequency-hopping binary frequency division multiplexing modulation signals of a known frequency-hopping pattern. Its main goal is to provide robust communications that can handle strong interferences, mostly in the setup of a communications network. Since the JANUS was accepted as the first standard for underwater acoustic communications, it is of interest to explore its performance in the presence of strong non-ambient interferences. The signals chosen are of an effective transmission rate of 100 bits per second at a carrier frequency of 12 kHz, and the frequency-hopping pattern lies between 8 and 16 kHz. The guard interval period between each modulation signal is chosen to be 2 ms. The transmitted sequence is of 9 s, and the information bearing bits are chosen uniformly at random.

For the narrowband interference, we use a constant single carrier waveform of frequency 12 kHz encoded by a random phase, which is randomized again every 1 s. This setup represents interference from the motor of a nearby vessel. Considering the case of a nearby vessel generating an interference chirp signal of a large source level, we test our system at the presence of an 8 s sequence of linear wideband chirp signals of frequency band 8—16 kHz and duration 30 ms, separated by a guard interval of 2 ms. This bandwidth covers the full frequency band of the chosen JANUS signals.

To test performance for different environments, we performed 1,000 Monte-Carlo simulations. In each simulation, we randomize the locations of the receiver, transmitter, and interferer within the map shown in Fig 8. The Depth map shows that the explored area included both a shallow water environment (depth of roughly 40 m), and a deeper water environment (depth of 180 m). The results are therefore applicable both to shallow water and to deeper water.

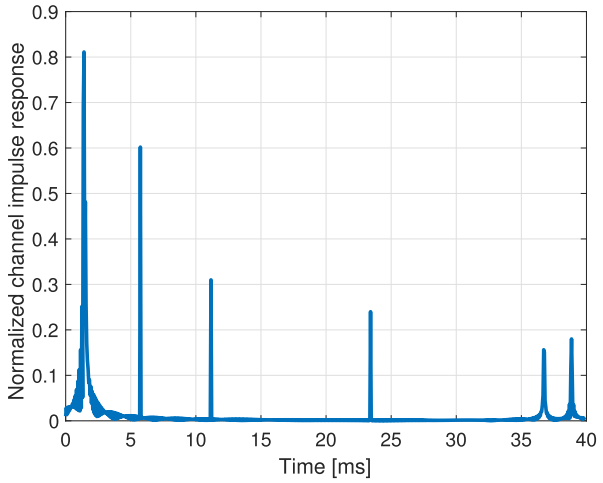

FIGURE 4. One example of a channel impulse response generated by the Bellhop simulator for a transmitter in 35 m of water and a receiver at water depth of 40 m.

The desired and interference signals are convolved with the simulated channels. These channels are constructed independently for the location pairs transmitter-receiver and interferer-receiver. For this, we adopt the ray-tracing model of the Bellhop propagation emulator [29]. A example of one of the channel impulse responses generated by the Bellhop simulator is shown in Fig. 4. A delay spread of about 40 ms is observed. The resulting signals are normalized, such that regardless of the locations selected, the SINR is set deterministically between -50 dB to -10 dB. The bellhop simulator we use assumes a frozen sea. That is, the channel is unrealistically time-invariant.[1] Still, since Bellhop is a widely accepted model, we use it to show robustness to different channel configurations, and provide results from sea experiments to cover this lack of practicality.

For each randomized location setup of the transmitter, receiver, and interferer, the simulated desired and interference signals are merged onto a single buffer. This buffer also includes a randomized ambient noise of zero mean i.i.d. Gaussian distribution. The noise level is chosen such that the SNR is 20 dB. We use a 10 s buffer. For the case of only narrowband interference, at the beginning 1 s of the buffer we place only the narrowband interference. The next 8 s include the desired signal with the addition of the narrowband interference. The last 1 s includes only the desired signal. In the case of wideband interference, we uniformly randomize the received time of the interference between 0 s and 2 s, such that interference can appear before, with, or after the reception of the desired signal. The result is a period of at least 1 s, where only the desired signal exists in the buffer. This allows us to compare the IC performance with the ideal case of no interference.

[1]Note that an extension of Bellhop called *Virtex* does offer some time-variation but is not used here.

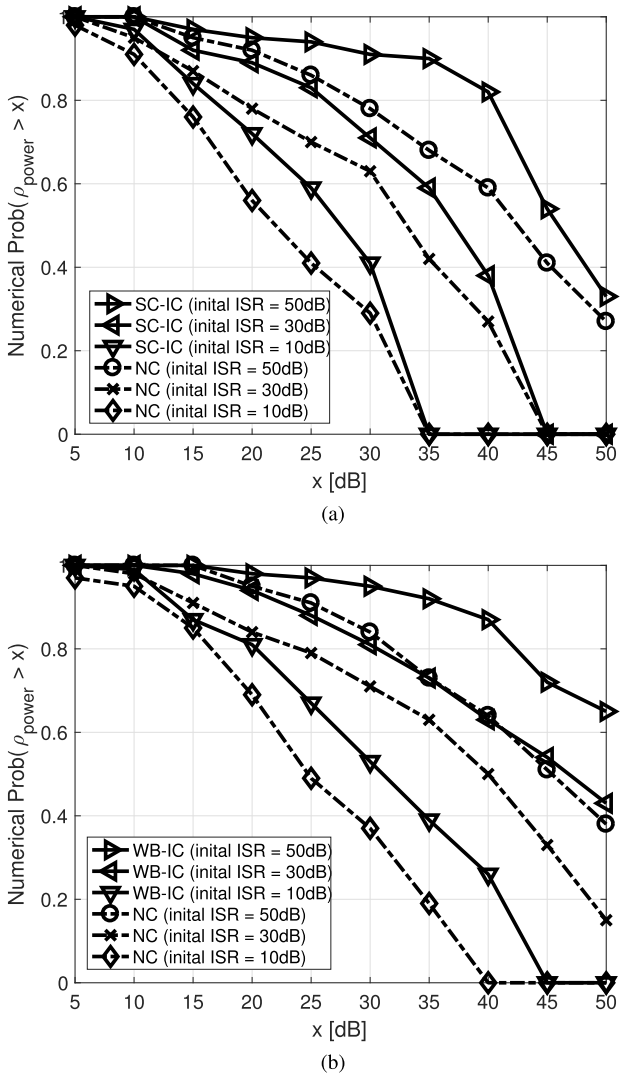

FIGURE 5. Empirical C-CDF of ρ_{power} for various SINR values. Signal is a sequence of linear 7–17 kHz chirp signals each of a 0.1 sec duration. Initial ISR is 30 dB, with an SNR of 20 dB. Interference is (a) single carrier at 12 kHz, (b) a sequence of linear 10–14 kHz chirp signals each of a 0.3 sec duration. Results show that both our SC-IC and BW-IC methods outperform the traditional adaptive noise cancellation method.

2) SIMULATION RESULTS

We start by analyzing the performance statistically, in terms of the complementary cumulative distribution function (C-CDF) of ρ_{power} as a function of the ISR. Since the C-CDF shows a probability measure, it has the benefit of showing the entire obtained results in a single figure. Thus, in contrast to average results, one can learn about the robustness of the method in different environmental settings. Results for narrowband interference and wideband interference are shown in Fig. 5a and Fig. 5b, respectively. The y-axis shows the numerical probability that the quality index is above a certain value x, and the x-axis represents this x value. For example, in Fig. 5a the y-axis is the numerical probability that the power measure is above level x, and x is given in dB in the x-axis. We observe that in all cases, our IC

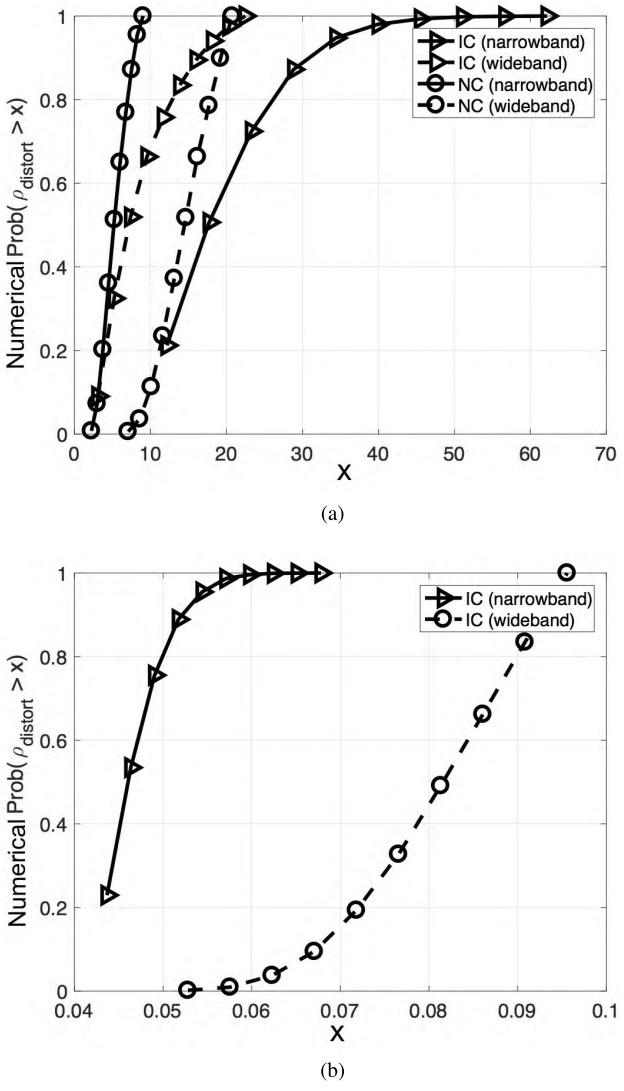

FIGURE 6. Empirical C-CDF of $\rho_{\text{distort}}(s(t))$. (a) NMF ratio with $s(t)$ being the desired signal, (b) NMF ratio with $s(t)$ being the interference signal. Initial ISR is 30 dB, with an SNR of 20 dB. Results show that the desired signal is much better received after the IC, and that the interference signal is well mitigated.

method performed much better than the NC benchmark. The results improve as the interference power increases. This is because the capability to track the significant taps improves as the interference becomes more observable. We also observe that the interference mitigation level is better for wideband interference compared to narrowband interference. This is because, in contrast to SC-IC, in WB-SC we assume knowledge of the signal's interference structure. Consequentially, the performance advantage of WB-SC over SC-IC increases with the interference's power.

Fig. 6a shows the C-CDF of the distortion ratio $\rho_{\text{distort}}(s(t))$ from (2), where $s(t)$ is the desired signal, and we consider both the narrowband and wideband interferences, as obtained by our SC-IC and WB-IC methods and by the NC benchmark. Results are shown for an ISR of 30dB before the IC. The results show that the NMF output has considerably increased for the desired signal. As we will show in the next section, for the sea experiment this NMF output is similar to the values obtained when no interference exists. That is, after the IC, the interference signal hardly affects the reception of the desired signal. With similar importance, from these results we conclude that our IC method does not distort the desired signal.

In Fig. 6b, we show the C-CDF of $\rho_{\text{distort}}(s(t))$, where $s(t)$ is the wideband interference signal. That is, we examine the amount of signal distortion experienced by the interference signal after the IC operation. Here, the desired outcome is a low $\rho_{\text{distort}}(s(t))$ level, which shows that the interference is mitigated after the IC. Indeed, we observe that for both the IC and NC approaches, a significant decrease in the NMF is obtained after the filtering operation. However, our IC approach outperforms the NC in terms of both value and robustness. The latter is evident from the narrower slope of the C-CDF obtained by BW-IC compared to the NC algorithm. From this, we conclude that the interfering signal has been successfully canceled.

Finally, we show the performance of our IC; as shown in Fig. 1, both SC-IC and WB-IC operate sequentially. This operational mode is suitable when the type of interference in the channel is not known. Performance is studied as a function of the bit-error-rate (BER) for four methods, namely, without IC (*No IC*); for the NC benchmark; SC-IC followed by WB-IC (*SC-WB*); and when the operating WB-IC is followed by the SC-IC scheme (*WB-SC*). We explore four cases: 1) no interference in the channel, 2) narrowband interference, 3) wideband interference, and 4) both narrowband and wideband interference in the channel. Average results are shown in Fig. 7. In all cases, the initial ISR is 30 dB, and the SNR is 10 dB.

Without interference in the channel, no significant difference is observed among the four methods. This is because, since the interference signal is assumed not to correlate well with the desired signal, the desired signal is not falsely identified as an interference by both the NC and our IC approaches. From this result, we conclude that our IC does not distort the desired signal. When either narrowband, wideband or both interferences exist, we observe that with no IC, communications is not possible. Comparing the performance of NC to our IC scheme, a significant benefit is observed in favour of our scheme, wherein the obtained gain over the benchmark is much greater for wideband interferences. This is because the frequency-hopping operation in the JANUS successfully handles single-carrier interference. Still, since the NC benchmark can barely handle wideband interference, the largest gain is obtained when both narrowband interference and wideband interference exist. The results show that, regardless of the interference type, no difference exists when operating SC-IC before WB-IC or vice versa. An interesting comparison is between the case of no interference (left bar in Fig. 7) and that of two types of interference (right bar in Fig. 7). Here, we observe that the BER obtained by our IC scheme is on the

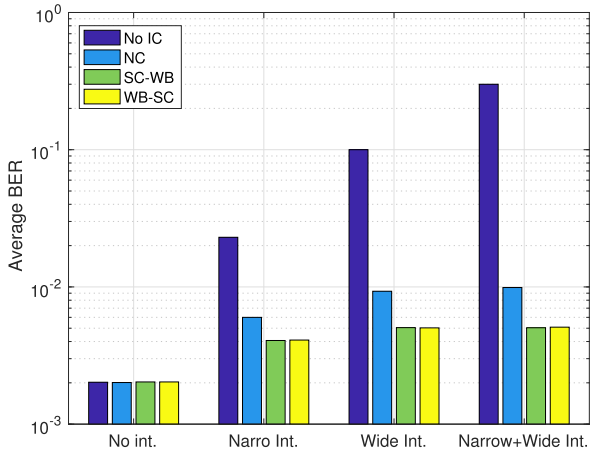

FIGURE 7. BER performance of the IC methods. Initial ISR is 30 dB. SNR is 10 dB. Results show good interference cancellation capability of our method for no interference, signal interference, or two types of interference.

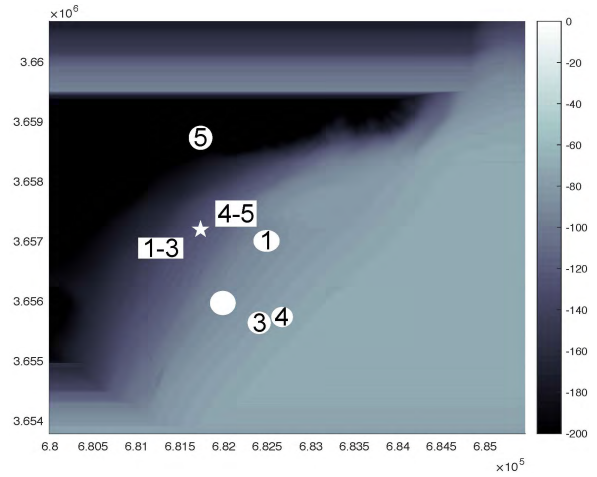

FIGURE 8. Bathymetry map from the sea experiment. Data is used for the Bellhop channel emulation. Horizontal and vertical axises are the 'x' and 'y' UTM coordinates. Locations of receiver is marked with a white star; positions of the transmitter and interferer during the five different tests are marked with white square and circle, respectively.

FIGURE 9. A picture of the communication floater and one of the transmitting vessels during the sea experiment.

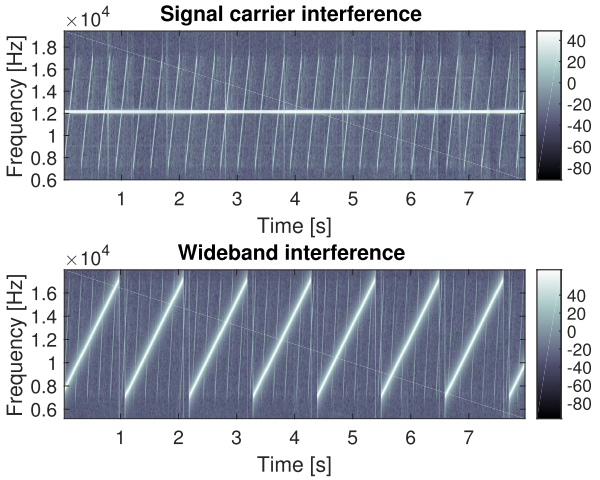

FIGURE 10. An example spectrogram of one received signal during the sea experiment. The upper figure shows a single carrier interruption at 12 kHz. The lower figure shows a sequence of 1 sec long 7–17 kHz linear chirps. The estimated SNR is 20 dB. The estimated ISR is 20 dB.

same order of magnitude with and without interference. That is, our IC scheme successfully removes the strong interference from the received signal.

B. SEA EXPERIMENT

To demonstrate the performance of our IC approach in a real environment, we performed a sea experiment. The experiment was performed on May 2017 in northern Israel in the area whose bathymetry is shown in Fig. 8 with a sea bottom of around 70 m. The bathymetry of the explored area is shown in Fig 8. We observe a large slope ranging from 60 m to 140 m. The data was collected using a Reson 400 kHz multibeam sonar. The upper-left side of the figure shows artificial data as bathymetry was not collected in the east-west side of the area.

The experiment included two vessels that served as a transmitter and an interferer, and an anchored communications floater, which served as the receiving node. A picture of the floating device and one of the transmitting ships is shown in Fig. 9. A total of 2,000 transmissions of individual chirp signals were performed over roughly two hours. Transmissions from the interfering and transmitter vessels were made at a source level of 180 dB Re 1μPa @1m and 150 dB Re 1μPa @1m, respectively. To allow for testing at different SINRs, the vessels moved in tandem with the anchored floater to create five different transmitter-receiver-interferer topologies. Throughout the experiment, the estimated SNR for the desired signal was above 20 dB. The measured sound speed was 1529 m/s with a water temperature of 21 degrees Celsius at the sea surface, and 1521 m/s with a water temperature of 17 degrees Celsius at the sea bottom with an approximately linear change. An example of the time-varying channel impulse response as evaluated from the recordings of the sea experiment is given in Fig. 2. The estimated delay spread is roughly 25 ms.

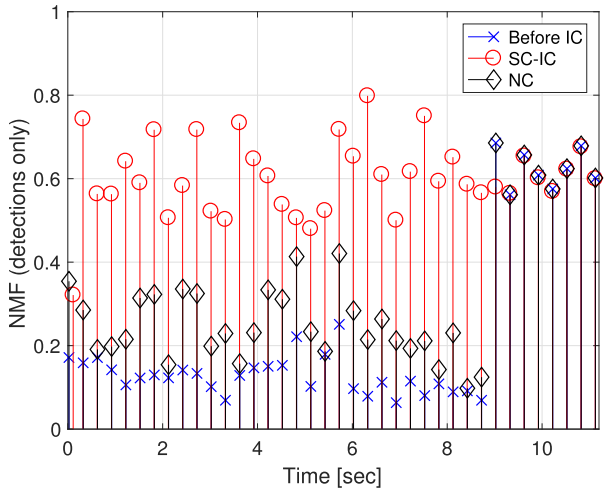

FIGURE 11. Sea experiment results with a normalized matched filter matched to the desired signal. (a) single carrier interference, (b) wideband interference. The results show a significant improvement in signal detection after IC, starting from the first symbol.

The desired signal was a sequence of linear chirp signals of a 0.1 sec duration, and a frequency band of 7—17 kHz. The narrowband interference was a constant sine wave with a carrier frequency of 12 kHz. The wideband interfering signal was another sequence of linear chirp signals at the same frequency band as the desired signal, but of a 1 sec duration. Examples of the received signals' spectrogram with wideband and narrowband interferences are shown in Fig. 10 for an initial ISR of 20 dB. Another example of a single buffer received during the experiment is shown in Figs. 11a and 11b for the NMF before the IC, using the SC-IC or the WB-IC, and using the NC benchmark. At the end of the buffer (from time 9 s), the received buffer included no interference. Hence, the NMF response corresponding to this period can be considered as the ideal case. We observe that before the IC, the NMF was very low and the interference overshadowed the reception of the received signal. Using the NC benchmark

TABLE 1. Sea Experiment results. The rows show different SINR levels. The columns show average interference mitigation for the two compared methods.

Initial ISR [dB]	SC-IC (single carrier interference)	NC (single carrier interference)	WB-IC (wideband interference)	NC (wideband interference)
40	52 dB	43 dB	56 dB	48 dB
30	41 dB	35 dB	46	38 dB
20	26 dB	16 dB	28 dB	18 dB
10	8 dB	2 dB	11 dB	4 dB
0	4 dB	0 dB	7 dB	1 dB

(represented by a black diamond curve), the results improve, but are still much lower than the ideal case with no interference (represented by a blue curve with an 'x' symbol at the end of the illustrated NMF response). That is, the interference mitigation is not complete. However, using our SC-IC and WB-IC (represented by a red circle curve), we observe that the NMF is very similar to the ideal case, i.e., the effect of the interference on the desired signal has been greatly reduced.

We tested the performance of both our SC-IC and WB-IC methods and compared them with those of the NC method. The results are described in Table 1 in terms of the SINR in the filter's output. The results reveal the dependency of both the IC and NC methods in the ISR. In particular, the filtering methods achieve good noise mitigation when the interference is well observed, i.e., when the initial ISR is high. That is, the noise mitigation technique mostly suits the case of strong interference. In particular, in the large initial ISR regime (above 20 dB), the noise mitigation is good. For these initial ISRs, the results show an improvement of 8-10 dB for our IC approach over the NC benchmark. This advantage reduces to about 4-7 dB for smaller initial ISR values. From these results, we conclude that our approach outperform the state-of-the-art methods in terms of noise mitigation for underwater acoustic signals, including a real sea environment.

VI. CONCLUSIONS

In this paper, we considered the problem of strong acoustics signals interfering with underwater acoustics applications like identification of sounds from marine mammals, signal detection, and underwater communications. We developed two interference cancellation algorithms: one for a single carrier interference, which does not require prior information about the interference, and one for a wideband interference of a known signal structure. Our algorithms were developed to converge rapidly, so as to manage the fast time-varying underwater acoustic channel. The algorithms were shown to be transparent from the perspective of the desired signal, and thus can be operated sequentially to manage both types of interferences. Numerical simulations for both chirp and communication signals show a much better interference mitigation capability for both algorithms compared to the traditional noise cancellation approach, and a similar trend was observed in a sea experiment for a chirp signal. Future research is necessary to improve the performance of the developed methods, including the low ISR region.

REFERENCES

[1] I. F. Akyildiz, D. Pompili, and T. Melodia, "Underwater acoustic sensor networks: Research challenges," *Ad Hoc Netw.*, vol. 3, no. 3, pp. 257–279, 2005.

[2] J. Zhang and Y. R. Zheng, "Frequency-domain turbo equalization with soft successive interference cancellation for single carrier MIMO underwater acoustic communications," *IEEE Trans. Wireless Commun.*, vol. 10, no. 9, pp. 2872–2882, Sep. 2011.

[3] R. Chassaing and D. Reay, "Adaptive filters," in *Digital Signal Processing*. Hoboken, NJ, USA: Wiley, 2008, pp. 319–353. [Online]. Available: http://ieeexplore.ieee.org/xpl/articleDetails.jsp?arnumber=5236581

[4] P. C. Etter, *Underwater Acoustic Modelling and Simulation*. Boca Raton, FL, USA: CRC Press, 2013.

[5] M. Shafi, S. Ogose, and T. Hattori, "Interference cancellation and multiuser detection," in *Wireless Communications*. Hoboken, NJ, USA: Wiley, 2002, pp. 291–316. [Online]. Available: http://ieeexplore.ieee.org/xpl/articleDetails.jsp?arnumber=5271045

[6] W. S. Burdic, *Underwater Acoustic System Analysis*. Los Altos, CA, USA: Peninsula, 2002.

[7] S. E. Cho, H. C. Song, and W. S. Hodgkiss, "Successive interference cancellation for underwater acoustic communications," *IEEE J. Ocean. Eng.*, vol. 36, no. 4, pp. 490–501, Oct. 2011.

[8] H. Ou, J. S. Allen, and V. L. Syrmos, "Frame-based time-scale filters for underwater acoustic noise reduction," *IEEE J. Ocean. Eng.*, vol. 36, no. 2, pp. 285–297, Apr. 2011.

[9] P. A. van Walree and R. Otnes, "Ultrawideband underwater acoustic communication channels," *IEEE J. Ocean. Eng.*, vol. 38, no. 4, pp. 678–688, Oct. 2013.

[10] J. C. Preisig, "Performance analysis of adaptive equalization for coherent acoustic communications in the time-varying ocean environment," *J. Acoust. Soc. Amer.*, vol. 118, no. 1, pp. 263–278, 2005.

[11] Y. R. Zheng, J. Wu, and C. Xiao, "Turbo equalization for single-carrier underwater acoustic communications," *IEEE Commun. Mag.*, vol. 53, no. 11, pp. 79–87, Nov. 2015.

[12] T. Riedl and A. Singer, "MUST-READ: Multichannel sample-by-sample turbo resampling equalization and decoding," in *Proc. IEEE OCEANS*, Jun. 2013, pp. 1–5.

[13] T. N. Zogakis, P. S. Chow, J. T. Aslanis, and J. M. Cioffi, "Impulse noise mitigation strategies for multicarrier modulation," in *Proc. IEEE Int. Conf. Commun. (ICC)*, vol. 2. May 1993, pp. 784–788.

[14] T. Li, W. H. Mow, and M. H. Siu, "Robust joint erasure marking Viterbi algorithm decoder," U.S. Patent 2009 0 052 594 A1, Feb. 26, 2009.

[15] X. Kuai, H. Sun, S. Zhou, and E. Cheng, "Impulsive noise mitigation in underwater acoustic OFDM systems," *IEEE Trans. Veh. Technol.*, vol. 65, no. 10, pp. 8190–8202, Oct. 2016.

[16] K. Pelekanakis, H. Liu, and M. Chitre, "An algorithm for sparse underwater acoustic channel identification under symmetric α-stable noise," in *Proc. IEEE OCEANS*, Jun. 2011, pp. 1–6.

[17] M. Morelli and M. Moretti, "Improved decoding of BICM-OFDM transmissions plagued by narrowband interference," *IEEE Trans. Wireless Commun.*, vol. 10, no. 1, pp. 20–26, Jan. 2011.

[18] N. I. Miridakis and D. D. Vergados, "A survey on the successive interference cancellation performance for single-antenna and multiple-antenna OFDM systems," *IEEE Commun. Surveys Tuts.*, vol. 15, no. 1, pp. 312–335, 1st Quart., 2013.

[19] Z. Wang, S. Zhou, J. Catipovic, and P. Willett, "Parameterized cancellation of partial-band partial-block-duration interference for underwater acoustic OFDM," *IEEE Trans. Signal Process.*, vol. 60, no. 4, pp. 1782–1795, Apr. 2012.

[20] S. Hadei and M. lotfizad. (Jun. 2011). "A family of adaptive filter algorithms in noise cancellation for speech enhancement." [Online]. Available: https://arxiv.org/abs/1106.0846

[21] A. Radosevic, T. M. Duman, J. G. Proakis, and M. Stojanovic, "Channel prediction for adaptive modulation in underwater acoustic communications," in *Proc. IEEE OCEANS*, Jun. 2011, pp. 1–5.

[22] S. G. Mallat and Z. Zhang, "Matching pursuits with time-frequency dictionaries," *IEEE Trans. Signal Process.*, vol. 41, no. 12, pp. 3397–3415, Dec. 1993.

[23] R. Diamant, A. Feuer, and L. Lampe, "Choosing the right signal: Doppler shift estimation for underwater acoustic signals," in *Proc. ACM Conf. Underwater Netw. Syst. (WUWNet)*, Los Angeles, CA, USA, Nov. 2012, p. 27.

[24] R. Diamant, "Closed form analysis of the normalized matched filter with a test case for detection of underwater acoustic signals," *IEEE Access*, vol. 4, pp. 8225–8235, 2016.

[25] K. C. H. Blom, H. S. Dol, A. B. J. Kokkeler, and G. J. M. Smit, "Blind equalization of underwater acoustic channels using implicit higher-order statistics," in *Proc. IEEE Underwater Commun. Netw. Conf. (UComms)*, Aug./Sep. 2016, pp. 1–5.

[26] F. Schulz, "Improvement of blind multichannel receivers for underwater acoustic communications by delay-based equalizer initialization," in *Proc. IEEE OCEANS*, May 2015, pp. 1–7.

[27] S. Haykin, *Adaptive Filter Theory*. Englewood Cliffs, NJ, USA: Prentice-Hall, 1996.

[28] J. Potter, J. Alves, D. Green, G. Zappa, I. Nissen, and K. McCoy, "The JANUS underwater communications standard," in *Underwater Commun. Netw. (UComms)*, Sep. 2014, pp. 1–4.

[29] M. Porter *et al. Bellhop Code*. Accessed: Nov. 2015. [Online]. Available: http://oalib.hlsresearch.com/Rays/index.html

ROEE DIAMANT received the B.Sc. and M.Sc. degrees from the Technion, Israel Institute of Technology, in 2002 and 2007, respectively, the Ph.D. degree from the Department of Electrical and Computer Engineering, University of British Columbia, in 2013. From 2001 to 2009, he was with the Rafael Advanced Defense Systems, Israel, as a Project Manager and Systems Engineer, where he developed a commercial underwater modem with network capabilities. In 2015 and 2016, he was a Visiting Professor with the University of Padova, Italy. He is currently the coordinator of the EU H2020 Project SYMBIOSIS (BG-14 track), and also leads the underwater Acoustic and Navigation Laboratory as an Assistant Professor with the Department of Marine Technology, University of Haifa. His research interests include underwater acoustic communication, underwater navigation, object identification, and classification. In 2010, he received the NSERC Vanier Canada Graduate Scholarship. In 2009, he received the Israel Excellent Worker First Place Award from the Israeli Presidential Institute. He received three best paper awards and also serves as an Associate Editor for the IEEE Ocean Engineering.